Proton Conducting Nanocomposite Membranes Based on Poly Vinyl Alcohol (PVA) / Glutaraldehyde (GA) for Proton Exchange Membrane Fuel Cells

Salehi Artimani, Javad; Ardjmand, Mehdi*[+]

Department of Chemical Engineering, South Tehran Branch, Islamic Azad University, Tehran, I.R. IRAN

Enhessari, Morteza

Department of Chemistry, Naragh Branch, Islamic Azad University, Naragh, I.R. IRAN

Javanbakht, Mehran[•]

Department of Chemistry, Amirkabir University of Technology, Tehran, I.R. IRAN

ABSTRACT: *In the present work, $BaCe_{0.85}Yb_{0.15}O_{3-\delta}$ mixed metal oxide nanoparticles supplying strong acid sites and good hydrophilic nature were used for the first time to build organic-inorganic proton exchange membranes. Poly(vinyl alcohol) - $BaCe_{0.85}Yb_{0.15}O_{3-\delta}$ (PVAYb) nanocomposite membranes were fabricated. Different analyses such as Scanning Electron Microscope (SEM), Energy Dispersive X-ray (EDX) spectroscopy, Fourier Transform Infra-Red (FT-IR) spectroscopy, and ThermoGravimetry Analysis (TGA) were used to characterize and study the structural properties of the obtained membranes. SEM and EDX analyses exhibited a homogenous dispersion of the nanoparticles in the nanocomposite membrane. It was found that $PVAYb_{1.5}$ had a better elemental distribution compared to $PVAYb_{2.5}$ composite membrane. PVAYb nanocomposite membrane containing 1.5 wt.% of $BaCe_{0.85}Yb_{0.15}O_{3-\delta}$ nanoparticles displayed a high proton conductivity value (64 mS/cm) at 70 °C operation temperature. The peak power density of 29 mW/cm^2 was obtained with a peak current density of 210 mA / cm^2 for as-prepared Proton Exchange Membrane Fuel Cell (PEMFC) equipped with $PPYb_{1.5}$ nanocomposite membrane at 70 °C.*

KEYWORDS: *PEMFC; Nanocomposite membrane; Proton conductivity; Poly(vinyl alcohol); Proton exchange membrane.*

INTRODUCTION

Proton exchange membrane fuel cells (PEMFCs) are known as interesting conventional power sources, because of their high energy efficiency and low pollution properties [1, 2]. Nafion perfluoro sulfonated ionomer is one of

* *To whom correspondence should be addressed.*

+ *E-mail: m_arjmand@azad.ac.ir*

● *Other Address : Fuel Cell and Solar Cell Laboratory, Renewable Energy Research Center, Amirkabir University of Technology, Tehran, I.R. IRAN*

1021-9986/2021/1/69-82 14/$/6.04

the most advanced commercially used membranes for PEMFCs application because of its good thermal and chemical stability, high proton conductivity and high mechanical strength [3].

In recent years, various Nafion-inorganic hybrid membranes have been reported by impregnating various hygroscopic oxide materials such as silica (SiO_2) [4], ceria (CeO_2) [5], zeolites [6] and also by incorporating other materials like graphene [7–9] and mesoporous carbon [10] into Nafion matrix. These hygroscopic nano fillers incorporated hybrid membranes showed improved hydration and resulted in higher cell performance under low RH values. In addition, incorporation of filler material improves the mechanical properties of hybrid membrane and contributes to inhibiting the direct permeation of reactant gases more by increasing the transport pathway tortuousness. However, Nafion use in PEMFCs is still restricted owing to the high cost, methanol crossover and operation at the temperatures less than 80 °C [11]. Therefore, fabricating the low-cost composite membranes with high protonic conductivity has been the challenge for researches to replace the commercial Nafion membrane with cheap membranes. Poly(vinyl alcohol) (PVA) is a hydrophilic, nontoxic, biocompatible and low cost polymer with excellent film-forming features. PVA films have good chemical stability, suitable mechanical strength and high potential for application in chemical crosslinking membranes [12,13]. However, high swelling and low protonic conductivity of PVA membranes limit their employment in PEMFCs [14]. *Kim et al.* reported that incorporation of TiO_2, ZrO_2 nanoparticles and zeolite into the PVA matrix enhance its water uptake and protonic conductivity properties [15]. Blending PVA with hydrophilic polymers such as Nafion, sPEEK and poly (styrene sulfonic acid-co-maleic acid) (PSSA-MA) is a proper route to achieve the above mentioned properties for PVA. Hydrophilic polymers can enhance the protonic conductivity of PVA-based membranes [16]. Besides, aldehyde and dialdehyde compounds have been used to crosslink PVA and control its mechanical stability [17]. Sulfonation agents, such as sulfoacetic acid and sulfosuccinic acid (SSA) are also used by some researchers to cross link of PVA for preparation of PVA-based membranes [18].

Recently, new proton conducting hybrid membranes have been introduced in polybenzimidazole/ionic liquids [19,20], polybenzimidazole/inorganic nanomaterials [21-24] and poly(vinyl alcohol)/$BaZrO_3$ [25] based PEM fuel cell systems. Perovskite structured protonic conductors have been studied practically due to their high chemical stability, excellent thermal and mechanical stability, relative low cost and high applicability in electrochemical devices for energy generation. So, understanding their proton transfer properties is necessary for evaluating the possibility to employ them in industrial scale method [26].

$BaCe_{0.85}Yb_{0.15}O_{3-\delta}$ is a proton conductor with a simple cubic perovskite structure and has a great potential in fuel cells because of its high levels of protonic conductivity [27-29]. $BaCe_{0.85}Yb_{0.15}O_{3-\delta}$ has been considered for applications in PEMFCs due to its low thermal conductivity, high chemical stability, extremely tolerant to vacancy formation and high structural and mechanical integrity even under excessive thermal excursions. ABO_3 perovskite-type oxides are structurally stable due to their well-balanced geometrical array of constituent atoms and their valences [30-33]. In ABO_3 structure, the A atom can be replaced with cations M^+ (Na, K), M^{2+} (Ca, Sr, Ba) or M^{3+} (Fe, La, Gd) and B atom can be replaced with M^{3+} (Mn, Fe, Co, Ga), M^{4+} (Ce, Zr, Ti) or M^{5+} (Nb, W) [34].

$BaCe_{0.85}Yb_{0.15}O_{3-\delta}$ is a refractory ceramic material with high melting point (2920 $^{\circ}$C) and low chemical reactivity. It is the only ceramic material that does not follow phase transitions over the temperature range from 269 ºC to 1327 ºC [27, 28].

In the present work, poly(vinyl alcohol)/$BaCe_{0.85}Yb_{0.15}O_{3-\delta}$ nanocomposite membranes were prepared by solution casting method. The structure, morphology, water uptake, thermal stability, proton conductivity and mechanical properties of the membranes were studied. $BaCe_{0.85}Yb_{0.15}O_{3-\delta}$ nanomaterial influence on proton conductivity and water uptake were also studied. Different analyses such as SEM, FTIR and TG analyses were used to characterize and study the physical properties of the obtained membranes.

EXPERIMENTAL SECTION

Materials

Poly(vinyl alcohol), 99+%, purchased from Merck Company. The cross-linking agent was a 25 wt.% of aqueous solution of glutaraldehyde (GA) which was aso purchased from Merck Company. All solvents were purchased from Sigma-Aldrich Company.

Synthesis of BaCeO3 nanoparticles

The synthesis procedure is according to ref. [35]. In a typical synthetic experiment, 0.197 g (1 mmol) of $BaCO_3$ (MW = 197 $gmol^{-1}$) was mixed with 0.548 g (1 mmol) of $(NH_4)_2Ce(NO_3)_6$ (MW = 548.23 g/mol) in a mortar and ground until a nearly homogeneous powder was obtained. The obtained powder was added into a 25 mL crucible and treated thermally in one step at 800 °C for 24 h in an electrical furnace. After the reaction was completed, the crucible was allowed to be cooled normally in the furnace to the room temperature. The obtained powder was collected for further analyses. The synthesis yield for $BaCeO_3$ (MW=325.45 $gmol^{-1}$) was 0.30 g (92 %) (S_1).

Synthesis of BaCe0.85Yb0.15O3-δ nanoparticles

The synthesis procedure was similar to that of pure $BaCeO_3$. Typically, 0.015 g (0.075 mmol) of Yb_2O_3, 0.197 g (1.00 mmol) of $BaCO_3$ and 0.470 g (0.95 mmol) of $(NH_4)_2Ce(NO_3)_6$ were mixed in a mortar and ground until a nearly homogeneous powder was obtained. The obtained powder was added into a 25 mL crucible and treated thermally in one step at 800 °C for 24 h (S_5). The crucible was then cooled normally in the furnace to the room temperature. A gray - like powder was obtained. The synthesis yield for $BaCe_{0.85}Yb_{0.15}O_{3-\delta}$ (MW=327.092 g/mol) was 0.30 g (92 %) (S_2).

Preparation of membranes

The PVA based membranes were made synthetically by dissolving proper amounts of PVA and $BaCe_{0.85}Yb_{0.15}O_{3-\delta}$ nanoparticle in deionized (DI) water under vigorous stirring at the temperature of 80 °C. Then GA was added gradually to the solution within 10 min. The resulting solution was stirred at 80 °C until a viscous solution was obtained. The final mixed solution was casted into petri-dishes and was air-dried for 1 day at room temperature until a solid membrane was achieved. When the membrane was dried, it was easily removed from the petri-dishes. The obtained nanocomposite membrane was then stored in DI water to be kept in hydrated form. The obtained PVA-$BaCe_{0.85}Yb_{0.15}O_{3-\delta}$ doped nanocomposite membrane was named $PVAYb_x$ according to x wt.% of the nanoparticles loaded in the membrane.

Water uptake and oxidative stability of membranes

The swelling amounts of the prepared membranes were investigated in the terms of their water uptake capabilities. Water uptake was measured according to the reference. In a typical experiment, a membrane was dipped in DI water for 1 day at room temperature. The wet membrane was removed from water, wiped with tissue papers and the wetted membrane weigh (W_{wet}) was determined instantly. The membrane was dried in an oven for 24 h at 80 °C and then weighted immediately to measure the dry membrane weight (W_{dry}). This process was repeated several times until a stable result was obtained. The water uptake was determined from equation (1).

$$\text{water uptake\%} = \frac{W_{et} - W_{dry}}{W_{dry}} \times 100 \quad (1)$$

Proton conductivity measurements

The proton conductivity of the membranes was calculated by the AC impedance spectroscopy using PGSTAT303N potentiostat/Galvanostat (Ecochemie). The sample membranes were dipped in DI water at room temperature for 1 day and then were sandwiched between two platinum electrodes. The measurements were performed in the potentiostatic mode. The resistance of the membranes was evaluated using impedance spectroscopy in the frequency range of 100 Hz – 1 MHz with signal voltage amplitude of 50 mV. The conductivity values were measured by using the below equation:

$$(\sigma = L / RS) \quad (2)$$

Where, σ, L, R, S refer to proton conductivity (S/cm), thickness (cm), resistance from the impedance data (Ω) and cross-sectional area (cm^2) of the membranes, respectively.

FT-IR ATR spectra

FTIR ATR spectra were acquired over the wavelength range from 600 to 4000 cm^{-1} using a Bruker Equinox 55 equipped with an attenuated total reflection accessory (ATR, single reflection). A resoloution of 4 cm-1 and 32 scans per sample were used.

SEM and EDX measurements

The morphology and chemical composition of the nanocomposite membranes was evaluated using

Scanning Electron Microscope (SEM), coupled with Energy Dispersive X-ray (EDX) spectroscopy (JEOL JSM 6390 LV scanning electron microscope, operating at an accelerating voltage of 15 kV).

Thermogravimetric analysis (TGA) and Mechanical Stability

Thermogravimetric analyses were carried out on a TGA/TA Instrument 2050 system at a heating rate of 20 °C/min from 25 to 600 °C.

To investigate the mechanical properties of membrabes , the mechanical features of the prepared dried membranes were measured by using Zwick/Roell Z030 testing machine. All the membranes were cut off to the standard shape and all the specimens were tested at speed of 10 mm/min and room temperature.

MEA and fuel cell tests

The Pt/C catalyst slurry ink used for of anode and cathode is composed of Pt-C powder (20 %), isopropyl alcohol (IPA), DI water and 15 wt.% Nafion binder solution (Aldrich). The resulting Pt-C ink was ultrasonicated for 1 h to disperse the catalyst powder and obtain a homogenous ink solution. The homogeneous Pt-C ink was coated on the carbon paper (containing MPL) by painting method. The loading amount was 0.5 mg/cm^2. The prepared electrodes were vacuum-dried in an oven at 80 °C for 30 min followed by further 120 °C for 60 min. The total Pt loading of each electrode was measured by the weight difference before and after painting process. Membrane electrode assembly (MEA) with 5 cm^2 active surface area was obtained by hot pressing cathode and anode; then, it was sandwiched with the $PVAYb_x$ nanocomposite membrane at 25 ºC less than 100 Kgf/cm^2 for 15 min. The flow of hydrogen and oxygen gases were maintained constant at 200 mL/min and 500 ml/min, respectively. Typical fuel cell polarization curves were recorded using a fuel cell evaluation system (FCT-150s) at 70 °C operation temperature.

RESULTS AND DISCUSSION

Water uptake and proton conductivity measurements

PVA based nanocomposite membranes were successfully obtained with 0.5-3.0 wt.% (0.5, 0.6, 0.7, 1.0, 1.2, 1.3, 1.5, 2, 2.5 and 3.0 wt.%) of $BaCe_{0.85}Yb_{0.15}O_{3-\delta}$ nanoparticles. $PVAYb_x$ nanocomposite membranes showed higher protonic conductivity compared to that of PVA based membrane (5.01×10^{-1} mS/cm) (Fig. 1). This increase was assigned to the hydrophilic feature of $BaCe_{0.85}Yb_{0.15}O_{3-\delta}$ nanoparticles in the PVA matrix.

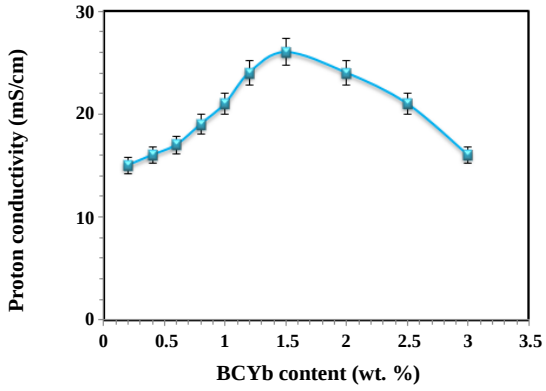

Fig. 1: Protonic conductivity of $PVAYb_X$ nanocomposite membranes at 25 °C.

The high protonic conductivity of $BaCe_{0.85}Yb_{0.15}O_{3-\delta}$ nanoparticles is due to the ability of the compound to dissolve protons of H_2O into their crystal system [27]. Protons are incorporated into $BaCe_{0.85}Yb_{0.15}O_{3-\delta}$ nanoparticles from water molecules to the nanoparticle surface, followed by diffusion into nanoparticle body by a dissociative absorption mechanism [28]. Schematic design of the proton transfer in the $PVAYb_{1.5}$ nanocomposite membranes are shown in Fig. 2.

$PVAYb_x$ nanocomposite membranes showed higher protonic conductivity compared to the PVA membranes. $BaCe_{0.85}Yb_{0.15}O_{3-\delta}$ nanoparticles had good hydrophilic nature and made strong hydrogen-bonding with water; so, they increased the water uptake and protonic conductivity of $PVAYb_x$ nanocomposite membranes. $PVAYb_{1.5}$ nanocomposite membranes displayed higher water uptake (220 %) and protonic conductivity (26 mS/cm) compared to PVA and other $PVAYb_x$ membranes at 25 °C. Similar results for water uptake amount were found in previous work. The results obtained from water uptake measurements indicated that $BaCe_{0.85}Yb_{0.15}O_{3-\delta}$ nanoparticles displayed a 9 % water uptake at 25 ˚C. This result confirms that $BaCe_{0.85}Yb_{0.15}O_{3-\delta}$ nanoparticles have hydrophilic nature.

The dependence of protonic conductivity to the operation temperature is shown in Fig. 3 for $PVAYb_{1.5}$ nanocomposite membrane. The figure indicates that

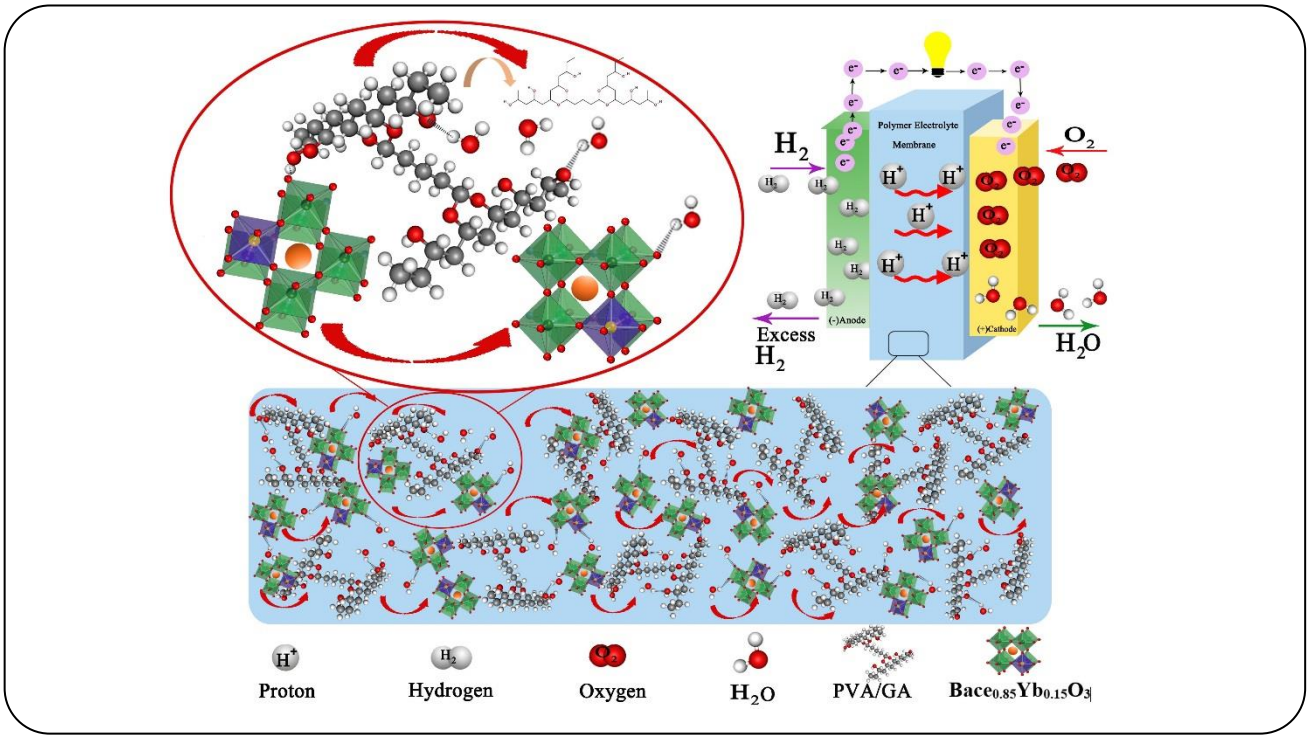

Fig. 2: Schematic illustration of the proton transfer mechanism in the PVAYb$_{1.5}$ nanocomposite membrane.

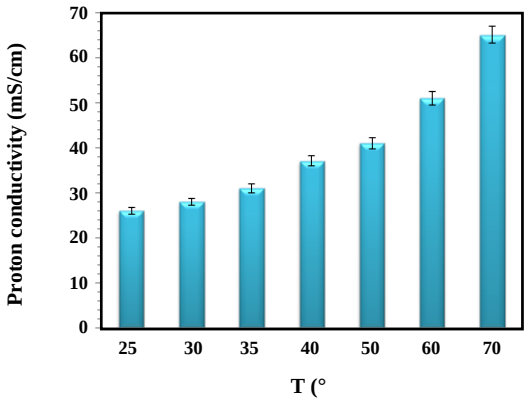

Fig. 3: Protonic conductivity of PVAYb$_{1.5}$ nanocomposite membrane at the different operation temperatures.

the protonic conductivity of the PVAYb$_{1.5}$ nanocomposite membrane is increased with increasing the operation temperature. The protonic conductivity values for PVAYb$_{1.5}$ nanocomposite membrane were 3.9 × 10^{-2} and 60.1 × mS/cm at 50 °C and 70 °C operation temperatures, respectively. The protonic conductivity is changed with changing the operation temperature in solid polymer electrolyte can be attributed to segmental (i.e., polymer chain) motion. The phenomenon increases the free volume of the system. So, it may allow the ions to jump or provide a pathway for ions to move from one site to another one. In other words, the segmental movement of the polymer facilitates the translational ionic motion.

Arrhenius and Vogel-Fulcher-Tammann (VFT) equations can be used to describe the relationship between the conductivity and temperature. The relationship between conductivities of ionic liquid and temperature followed Arrhenius equation [39], which is described as

$$\ln\sigma = \ln\sigma_{\infty}\exp(-E\sigma / RT) \quad (1)$$

Where, σ is the conductivity and σ_{∞} is the empirical constant. E_{σ} notes for the activation energy. T is the temperature and R is 8.314 J/mol·K. Also, According to [40], the conductivity of ionic liquids also obeyed Vogel-Fulcher-Tammann (VFT) equation which is shown in

$$\sigma = \sigma_0 \exp(-B/(T - T0)) \quad (2)$$

Where, σ_0, B, and $T0$ are the empirical constants. According to the Arrhenius and VFT equations, the relationship between conductivity and temperature is shown in Fig. 4(a) and 4(b), respectively; corresponded parameters are calculated and listed in Table 1.

Table 1: Fitting parameters for the Arrhenius and Vogel–Fulcher–Tammann equations.

Membrane	Arrhenius equation			VFT equation			
	σ_{∞} (mS/cm)	E_a (Kj/mol)	R^2	σ_0 (mS/cm)	B (K)	T_0 (K)	R^2
$PVAYb_{1.5}$	25363.08375	17.111	0.988	151.59007	295.793	255	0.998

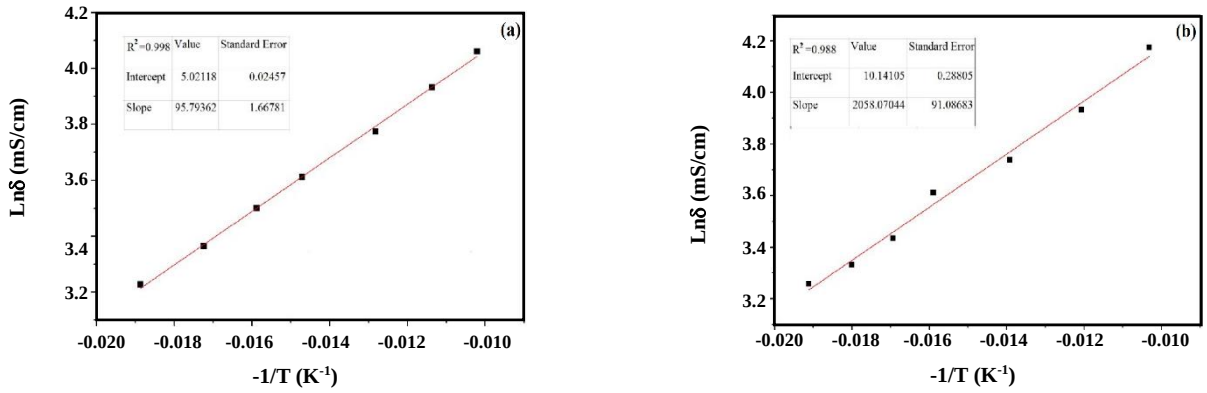

Fig. 4: (a) Arrhenius and (b)VFT plots for protonic conductivity of $PVAYb_{1.5}$ nanocomposite membrane.

From Table 1, it is clearly seen that VFT equation (R^2=0.998) is better to describe the relationship between conductivity and temperature than Arrhenius equation (R^2=0.988).

Table 2 displays a comparison study among the protonic conductivity property of the nanocomposite membrane at different operation temperatures reported in the present and the other published works [41-47]. It shows that $PVAYb_{1.5}$ nanocomposite membrane confirms a significant protonic conductivity (64 mS/cm at 70 °C) compared to other PVA nanocomposite membrane. The considerable protonic conductivity value for $PVAYb_{1.5}$ nanocomposite membrane can be attributed to the excellent proton transfer mechanism in the $BaCe_{0.85}Yb_{0.15}O_{3-\delta}$ crystal system which enhances the proton transfer pathways and also, strengthens the hydrogen-bonding between $BaCe_{0.85}Yb_{0.15}O_{3-\delta}$ nanoparticle and water molecule. The results show that the water uptake amount for the synthesized nanocomposite membrane is higher than that of the commercial Nafion 117 membrane; so the protonic conductivity of the ass-prepared membrane is comparable to the Nafion 117 membrane.

$BaCe_{0.85}Yb_{0.15}O_{3-\delta}$ nanoparticles have chemical interactions with the environment due to their high surface energy. So, they are extremely unstable. Hence, their self-aggregation leads to a decrease in their specific surface area, water uptake and protonic conductivity. So, $BaCe_{0.85}Yb_{0.15}O_{3-\delta}$ nanoparticles content in the membrane that is a key parameter for manufacturing the nanocomposite membrane is investigated in the present study. Fig. 1 shows that introducing large amount (more than 1.5 wt %) of $BaCe_{0.85}Yb_{0.15}O_{3-\delta}$ nanoparticles decreases the protonic conductivity of $PVAYb_x$ nanocomposite membranes. These results can be attributed to the self-aggregation of the nanoparticles inside the membranes.

In the Grotthus mechanism for proton transfer in $BaCe_{0.85}Yb_{0.15}O_{3-\delta}$ nanoparticles, proton diffuses by an arrangement around the oxygen and jumps from an oxygen to a nearest neighbor ion [36,37]. The O-H groups orient toward H^+ ions which are belonged to the neighbor oxygen atoms. The rotation period (10–12 s) and jumping time (~9–10 s) is low; so it is considered as the limiting step in the conduction mechanism. The strong interaction between the proton and the two oxygen neighbors supplies enough energy to break the O-H bond. During the process, a nonstoichiometric perovskite material such as oxygen-deficient $ABO_{3-\delta}$, A-deficient $A_{1-\delta}BO_3$, or B-deficient $AB_{1-\delta}O_3$ is exist; δ is the number of deficient atoms per unit formula. In the first case, an oxygen vacancy is formed. So, hydroxide group from water dissociation fills

Table 2: A comparison study of protonic conductivity for several of nanocomposite PVA membranes.

Modifier	T (°C)	Proton conductivity (mS/cm)	Ref.
$PVAYb_{1.5}$	70	64	Present work
Nafion117	25	13.4	[41]
Nafion117	80	62	[42]
PVA/PVP/$BaZrO_3$ (1wt%)	70	0.60	[43]
PVA/$La_2Ce_2O_7$ (4wt%)	25	19	[44]
PVA/SSA/PVP*	25	14	[45]
PVA/ZIF*	60	0.20.4	[46]
PVA/ODADS*	71	42.4	[47]

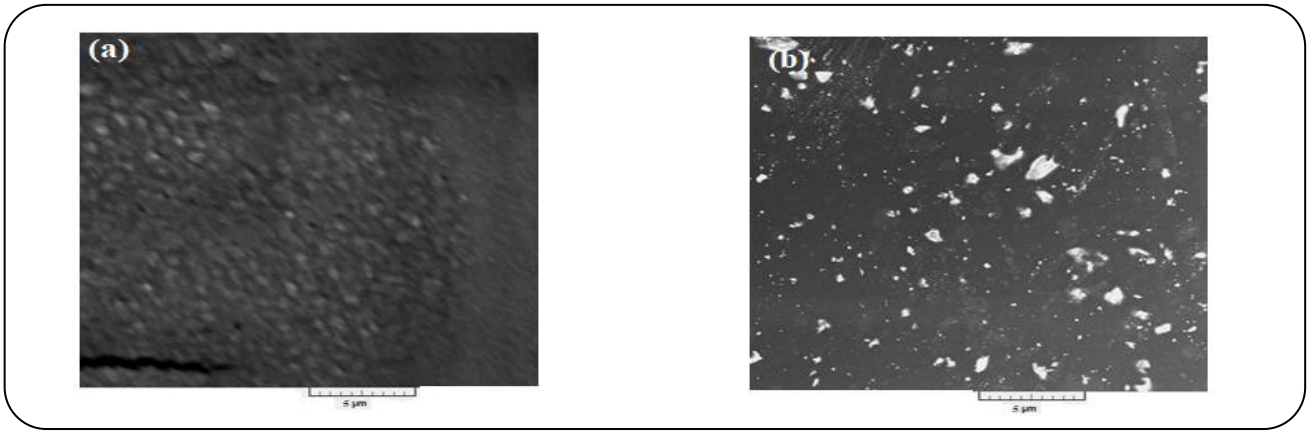

Fig. 5: SEM images of the cross-section of (a) $PVAYb_{1.5}$ and (b) $PVAYb_{2.5}$ nanocomposite membranes.

the vacant oxygen site, whereas the incorporated proton forms chemical bonding to the lattice oxygen in the nanoparticle crystal system [38].

Fig. 5 shows the cross-sectional SEM images of $PVAYb_{1.5}$ (a), and $PVAYb_{2.5}$ (b) nanocomposite membranes. Fig. 5a indicates that the particle size distribution of the prepared $PVAYb_{1.5}$ nanocomposite membrane is homogenous. Significant agglomerations of $BaCe_{0.85}Yb_{0.15}O_{3-\delta}$ nanoparticles were clearly visible in the $PVAYb_{2.5}$ nanocomposite membranes (Fig. 5b). The image indicates that the aggregation of $BaCe_{0.85}Yb_{0.15}O_{3-\delta}$ nanoparticles is occurred when the amount of the nanoparticles in the membrane is increased. The agglomeration decreases the active surface area of the nanoparticles in the membrane and accordingly the membrane water uptake amount is decreased.

FT-IR ATR spectra

Fig. 6 shows typical ATR spectrum for $PVAYb_{1.5}$ nanocomposite membrane. The broad bands at around 3200-3600 cm^{-1} are assigned to hydrogen bonding and -OH vibration [48,49]. The high intensity of the -OH peak in the $PVAYb_{1.5}$ nanocomposite membrane compared to PVA membranes is because of the existence of hydrogen bonding among $BaCe_{0.85}Yb_{0.15}O_{3-\delta}$ nanoparticles and water molecules. The bands at 2907 cm^{-1} and 1324-1422 cm^{-1} are attributed to the C-H stretching and bending vibrations of methylene groups, respectively. The peak at 2850 cm^{-1} shows the presence of aldehyde group [50]. The peak at 1720-1730 cm^{-1} is also assigned to C=O group. However, it is covered apparently by vicinity band in the region [51,52]. The peak at 1000 cm^{-1} is assigned to the C-O group of PVA based membrane. The bands at 1200-1250 cm^{-1} are attributed to the C-O-C bonds formed from the reaction between OH group with -CHO group in GA [47].

Thermal properties

Fig. 7 shows that $PVAYb_{1.5}$ nanocomposite membrane has a higher thermal stability compared to PVA membrane.

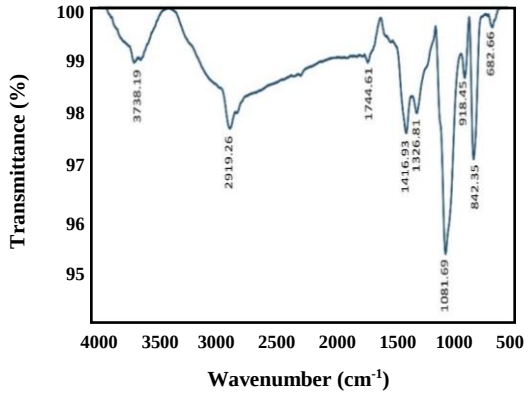

Fig. 6: FT-IR ATR spectrum of PVAYb$_{1.5}$ nanocomposite membrane.

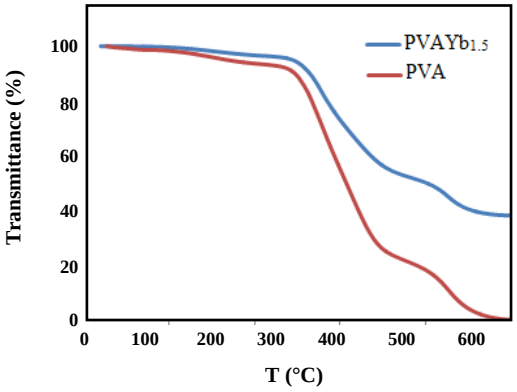

Fig. 7: TGA plots of PVA and PVAYb$_{1.5}$ nanocomposite membranes.

Incorporation of $BaCe_{0.85}Yb_{0.15}O_{3-\delta}$ nanoparticles in PVA polymer matrix increases the decomposition temperature of the prepared nanocomposite membrane compared to PVA membrane. Among the perovskites with cubic structures, $BaCe_{0.85}Yb_{0.15}O_{3-\delta}$ is an actual promising ceramic material due to its high melting point (2920 ºC) and low chemical reactivity with corrosive compounds. Unlike most of the perovskite systems, $BaCe_{0.85}Yb_{0.15}O_{3-\delta}$ does not undergo any (long-range-order) structural phase transition. In addition, $BaCe_{0.85}Yb_{0.15}O_{3-\delta}$ shows an excellent thermal stability due to the low thermal expansion coefficient ($\alpha = 87 \times 10^{-7}$/ ºC in the range of 25 ºC to 1080 ºC).

GA is a cross linking agent, can compact and rigid the PVA structure and decrease the free volume for up taking water molecules [47]. However, it increases the thermal stability of the nanocomposite membrane compared to PVA based membrane. $BaCe_{0.85}Yb_{0.15}O_{3-\delta}$ nanoparticles have excellent hydrophilic property and improve the thermal stability and water uptake properties when are added into the membrane in appropriate amount.

Generally, A PEMFC has a working temperature from 60 to 100 °C and an efficiency of about 50 %, such that the remaining 50 % is waste heat. The waste heat must be discharged efficiently from the fuel cell to protect the proton exchange membrane. All the as prepared membranes have good thermal stability in the mentioned operation temperature range. However, TGA plots at the temperatures more than 100 °C show that the thermal stability of the PVAYb$_{1.5}$ membranes is improved due to the existence of $BaCe_{0.85}Yb_{0.15}O_{3-\delta}$ nanoparticles in the membrane. PVAYb$_{1.5}$ nanocomposite membrane displays a higher thermal stability than PVA membranes due to the high polarity of $BaCe_{0.85}Yb_{0.15}O_{3-\delta}$ nanoparticles because of making strong hydrogen-bonding with PVA and intense intra-molecular interaction. The high thermal stability of the as-prepared PVAYb$_{1.5}$ nanocomposite membrane confirmed its capability for employing in high temperatures PEMFCs applications.

Mechanical properties

Tensile strength, elongation at break point and modulus of elasticity were obtained using a SSTM-5KN mechanical testing machine (Iran). Uniaxial stress–strain and ultimate properties were performed on 5 mm × 30 mm^2 samples with various percentages of BaCe0.85Yb0.15O3-δ nanoparticles (0-1-1.5-2-2.5). Each film was placed between the jaws of the device. The initial distance between the jaws and the velocity of the maxillary jaw was 30 mm and 3 mm / min, and then stress and strain were recorded using a computer. Stress–strain curves plotted in Fig. 8 were obtained from experimental data as close as possible to the mean mechanical properties. The average and standard deviation of the mechanical properties of membranes are presented in the Table 3.

As can be seen from table, the modulus of elasticity and tensile strength of membranes in all nanoparticle percentages increased significantly so that the highest tensile strength and modulus of elasticity are related to the PVAYb1.5 membrane. However, with increasing nanoparticle percentage, tensile strength and modulus of elasticity of membranes decreases. Increase in tensile

Table 3: Typical Tensile Strength, Elongation, and Tensile Modulus of prepared membranes.

Samples	Tensile Strength (MPa)	Modulus of elasticity (GPa)	Elongation at break (%)
PVA	60±1	2.1±0.3	3.2±0.1
$PVAYb_1$	90±1	3.3±0.3	2.2±0.4
$PVAYb_{1.5}$	106.9±1.9	5.1±0.2	2.1±0.2
$PVAYb_2$	84.03±1	4.6±0.4	1.86±0.2
$PVAYb_{2.5}$	73±1.98	3.5±0.6	1.08±0.4

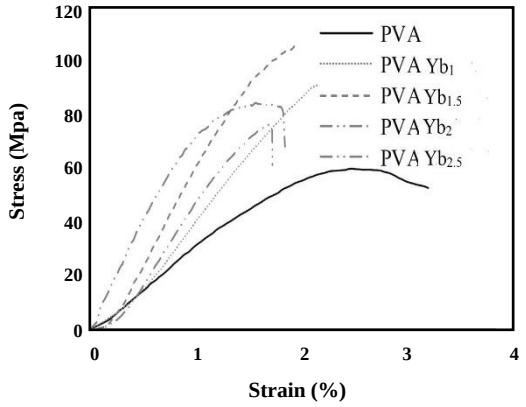

Fig. 8: Mechanical stability plot of as-prepared PVA –based nanocomposite membranes.

strength and modulus of elasticity in less nanoparticle percentages is probably due to the strong surface bond between nanoparticle and PVA matrix, which results in the effective transfer of stress from the polymer matrix and uniform nanoparticle dispersion in the matrix and more compatibility between the nanoparticles and the polymeric network, and the reduction of mechanical properties of membranes with more than 1.5% nanoparticles are probably due to the accumulation of nanoparticles and poor surface adhesion between polyvinyl alcohol and nano-particle

Dispersion of the Ba, Ce and Yb nanoparticles in the cross-section of $PVAYb_{1.5}$ nanocomposite membrane was investigated by the EDX mapping images (Fig. 9 a,a′). The EDX images confirm the homogeneity of the distribution of Ba and Ce particles in the $PVAYb_{1.5}$ nanocomposite membrane is more than $PVAYb_{1.5}$ nanocomposite membrane (Fig. 9 b,b′). Uniform dispersion of nanoparticles in the $PVAYb_{1.5}$ nanocomposite membranes increases the PVA-nanoparticles interactions and improves its mechanical stability. So, according to the above mentioned discussion, $PVAYb_{1.5}$ nanocomposite membrane is adequate to be fabricated into membrane electrode assemblies.

Fuel cell performance

The as-prepared $PVAYb_{1.5}$ nanocomposite membrane was used for its performance assessment in non-humidified H_2/O_2 PEMFCs by building membrane electrode assemblies (MEAs). The anode and cathode weights were 0.5 mg/cm^2 (active area = 5 cm^2). The PEMFC unit cell performance of these MEAs were tested at 25, 50, and 75 °C under ambient pressure with non-humidified H2/O2 flows. Fig. 10 depicts current density versus cell voltage curves for the PEMFCs using $PVAYb_{1.5}$ nanocomposite membranes at 25°C, 50°C and 70 °C at dry conditions. The $PVAYb_{1.5}$ nanocomposite membrane exhibits power performance of 9.48 mW/cm^2 with a current density of 59 mA/cm^2 at 25 °C operation temperature. Also, the maximum power density (29 mW/cm^2) is observed with a peak current density of 210 mA/cm^2 for $PVAYb_{1.5}$ membrane at 70 °C operation temperature at dry condition. As can be seen, increasing the temperature significantly improved the fuel cell performance. Increasing the power density of $PVAYb_{1.5}$ nanocomposite membrane with increasing the operation temperature is owing to the higher protonic conductivity property of the membrane. Consequently, the high protonic conductivity of $PVAYb_{1.5}$ membranes improves the conversion of the fuel to the electrical power through a redox process in the fuel cell and so enhances the power density of the fuel cell.

Open circuit voltage (OCV) is determined in the absence of any current flux in the fuel cell. This condition is known as the initial voltage before measuring the voltage of the pulse. The open circuit voltage for as-prepared membranes was about 0.93 V at 70 ° C. The polarization plot can be classified into different regions: an additional voltage activation (initial voltage drop),

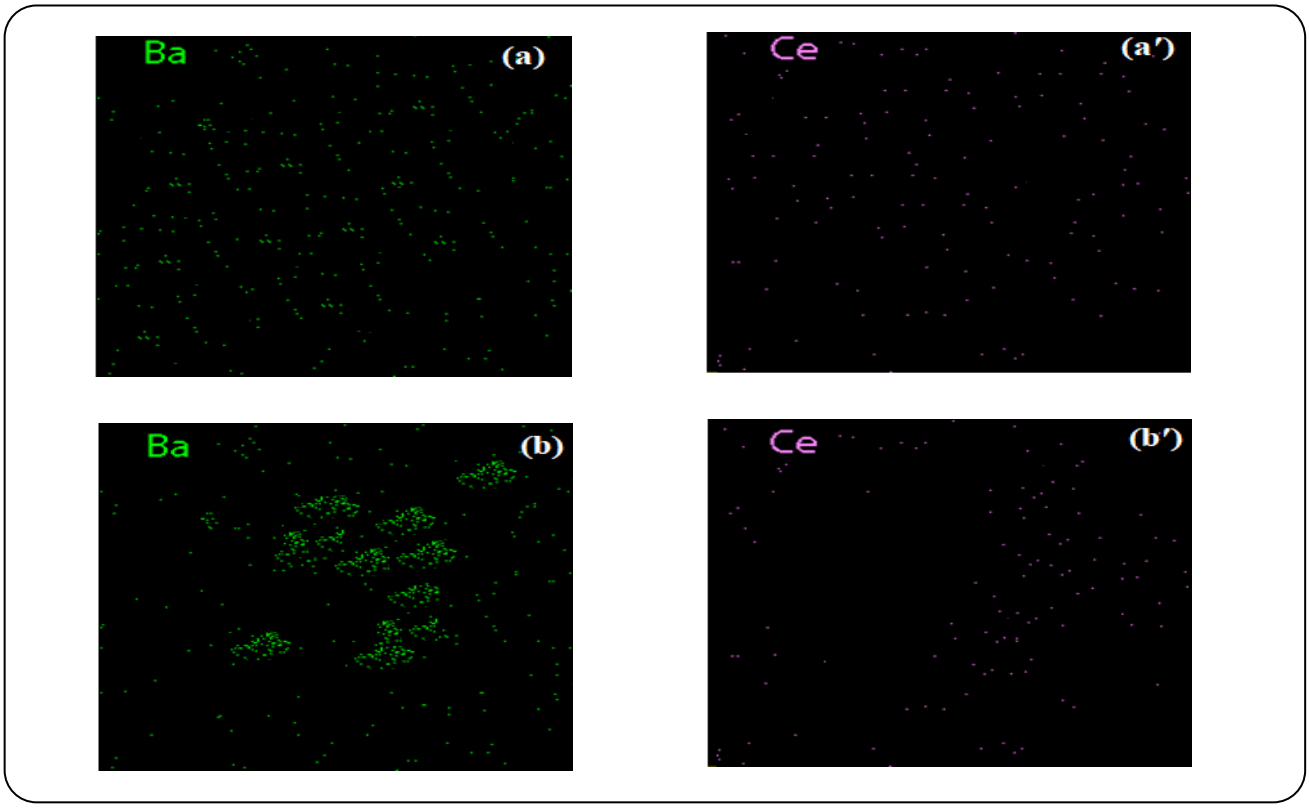

Fig. 9: EDX images showing the distribution of Ba and Ce particles in the cross-section of PVAYb$_{1.5}$ (a,a') and PVAYb$_{2.5}$ (b,b') nanocomposite membranes.

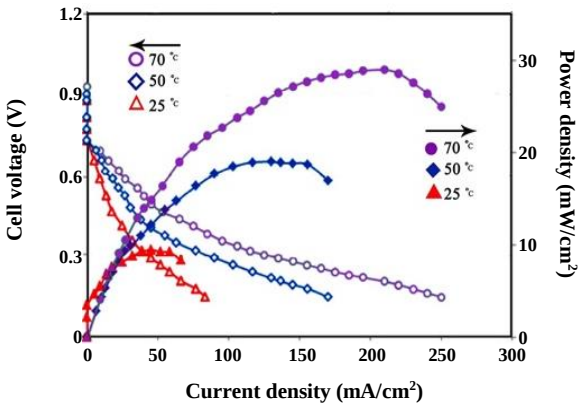

Fig. 10: Current density versus cell voltage curves of PVAYb$_{1.5}$ nanocomposite membranes at different temperatures.

an additional ohmic voltage, and an additional concentration voltage. The additional activation voltage with a barrier to energy prevents the chemical reaction between reactants. Additional voltage activation is the main source of voltage drop when the current density is assisted. In medium and low temperature fuel cells, the additional activation voltage is the most important irreversible and voltage drop factor. The additional activation voltage at lower temperatures and pressures is less important. Ominous excess voltage occurs due to resistance loss in the cell. The additional concentration voltage is the pressure drop from reactive starvation. Indeed, the initial drops of the same voltage with different membranes, electrodes, and MEA procedures were determined when the same instrument was used (a drop of 150-200 Mv without change directly after applying the load). Increasing the power density of nanocomposite membranes PVAYb1.5 is potent due to increased temperature owing to higher proton potentials. As a result, the high conductivity of the proton nanocomposite membranes improves the conversion of fuel to electricity through the oxidation-reduction process in the fuel cell system, thereby increasing the density of the fuel cell power.

EIS spectra analysis

Fig. 11(a and b) represents the Nyquist and Bode modulus plots, respectively, for PVA and PVAYb1 and

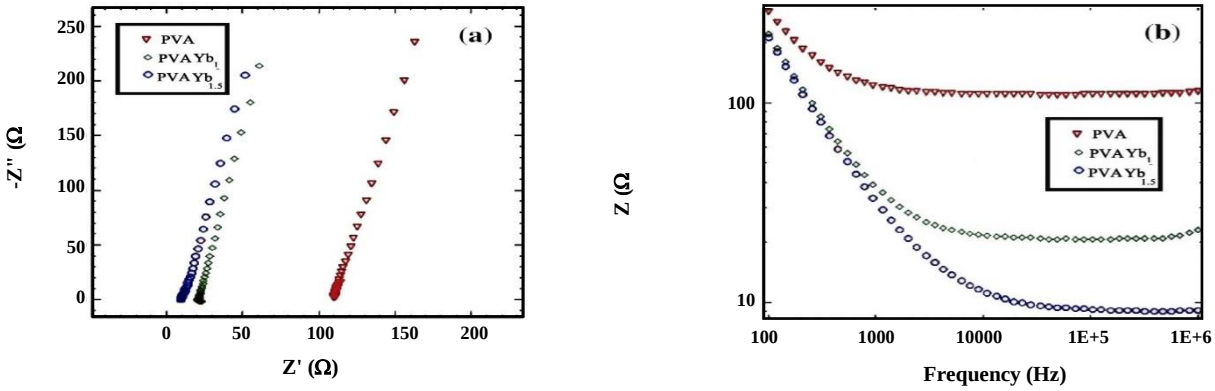

Fig. 11: Nyquist (a) and Bode modulus (b) plots for PVA and PVAYb1 and PVAYb1.5 membranes at 25 ° C.

PVAYb1.5 membranes at 25 ° C. According to Fig (a), the PVAYb1.5 nanocomposite membranes showed more proton conductivity compared to PVAYb1 and PVA membranes. Bode Modulus plots (b) showed that PVAYb1.5 has Lowest resistance among nanocomposite membranes which is in accordance to Nyquist plots. Bode Modulus plots also show that the lowest resistance is observed at the highest frequency. Therefore, based on the equation ($\sigma = L / RS$), low frequency resistors were used in the Nyquist plot to achieve proton conductivity.

CONCLUSIONS

Solution casting method was employed for preparation of advanced nanocomposite membrane based on PVA/ $BaCe_{0.85}Yb_{0.15}O_{3-\delta}$. PVA and $BaCe_{0.85}Yb_{0.15}O_{3-\delta}$ were used as the based polymer and inorganic modifier agent, respectively. Glutaraldehyde (GA) was used as PVA-crosslinker. The nanocomposite membrane showed a higher water uptake and protonic conductivity compared to those of the PVA based membrane when the amount of $BaCe_{0.85}Yb_{0.15}O_{3-\delta}$ nanoparticle was 1.5 wt %. The observation was due to the strongly hydrophilic character of $BaCe_{0.85}Yb_{0.15}O_{3-\delta}$ nanoparticles. PVA/ $BaCe_{0.85}Yb_{0.15}O_{3-\delta}$ nanocomposite membrane (with 1.5 wt % of nanoparticle) displayed a protonic conductivity of 64 mS/cm at 70 °C. The strong surface interactions of $BaCe_{0.85}Yb_{0.15}O_{3-\delta}$ nanoparticles increased the mechanical properties of the nanocomposite membrane. SEM and EDX analyses exhibited a homogenous dispersion of the nanoparticles in the nanocomposite membrane. The electrochemical performance of PVA/ $BaCe_{0.85}Yb_{0.15}O_{3-\delta}$ nanocomposite membranes (1.5 wt.% of $BaCe_{0.85}Yb_{0.15}O_{3-\delta}$ nanoparticle) was found to be 29 mW/ cm^2 at 70 °C. The results of protonic conductivity measurements and fuel cell tests exhibited the best properties of PVA/ $BaCe_{0.85}Yb_{0.15}O_{3-\delta}$ nanocomposite membrane among the numerous explored compositions and propose it as a promising candidate for electrolyte in fuel cell devices.

Received : Mar. 6, 2019 ; Accepted : Sep. 23, 2019

REFERENCES

[1] Mandanipour V., Noroozifar M., Modarresi-Alam A.R., Khorasani-Motlagh, M., Fabrication and Characterization of a Conductive Proton Exchange Membrane Based on Sulfonated Polystyrenedivinylbenzene Resin-Polyethylene (SPSDR-PE): Application in Direct Methanol Fuel Cells, *Iran. J. Chem. Chem. Eng. (IJCCE)*, **36(6)**: 151-162 (2017).

[2] Ahmadizadegan H., Esmaielzadeh S., Ranjbar M., Improving the Proton Conductivity and Antibacterial Properties of Sulfonated Polybenzimidazole/ZnO/Cellulose with Surface Functionalized Cellulose/ZnO Bionanocomposites, *Iran. J. Chem. Chem. Eng. (IJCCE)*, **37(4)**: 27-42 (2018).

[3] Tian A.H., Kim J.-Y., Shi J.Y., Lee K., Kim K., Surface-modified Nafion Membrane by Trioctylphosphine-Stabilized Palladium Nanoparticles for DMFC Applications, *J. Phys. Chem. Solids*, **70(8)**: 1207-1212 (2009).

[4] Bae I., Oh K.H., Yuan S.H., Kim H., Asymmetric silica Composite Polymer Electrolyte Membrane for Water Management of Fuel Cells, *J. Membr. Sci.*, **542**: 52–59 (2017).

[5] Velayutham P., Sahu A.K., Parthasarathy S., A Nafion-Ceria Composite Membrane Electrolyte for Reduced Methanol Crossover in Direct Methanol Fuel Cells, *Energies*, **10(2)**: 259 (2017).

[6] Devrim Y., Albostan A., Enhancement of PEM Fuel Cell Performance At Higher Temperatures and Lower Humilities by High Performance Membrane Electrode Assembly Based on Nafion/Zeolite Membrane, *Int. J. Hydrog. Energy*, **40(44)**: 15328–15335 (2015).

[7] Peng K.-J., Lai J.-Y., Liu Y.-L., Nanohybrids of Graphene Oxide Chemically-Bonded with Nafion: Preparation and Application for Proton Exchange Membrane Fuel Cells, *J. Membr. Sci.*, **514**: 86–94 (2016).

[8] Sahu A.K., Ketpang K., Shanmugam S., Kwon O., Lee S., Kim H., Sulfonated Graphene–Nafion Composite Membranes for Polymer Electrolyte Fuel Cells Operating Under Reduced Relative Humidity, *J. Phys. Chem. C.* **120(29)**: 15855–15866 (2016).

[9] Parthiban V., Akula S., Peera S.G., Islam N., Sahu A.K., Proton Conducting Nafion Sulfonated Graphene Hybrid Membranes for Direct Methanol Fuel Cells with Reduced Methanol Crossover, *Energy Fuels*, **30(1)**: 725–734 (2016).

[10] Sasikala S., Selvaganesh S.V., Sahu A.K., Carbone A., Passalacqua E., Block Copolymer Templated Mesoporous Carbon–Nafion Hybrid Membranes for Polymer Electrolyte Fuel Cells Under Reduced Relative Humidity, *J. Membr. Sci.*, **499**:503–514 (2016).

[11] Yin C., Wang Z., Luo Y., Li J., Zhou Y., Zhang X., Zhang H., Fang P., He C., Thermal Annealing on Free Volumes, Crystallinity and Proton Conductivity of Nafion Membranes, *J. Phys. Chem. Solids*, **120**: 71-78 ( ).

[12] Hassan S., Yasin, T., Imran Z., Batool S.S., Silane Based Novel Crosslinked Chitosan/Poly(Vinyl Alcohol) Membrane: Structure, Characteristics and Adsorption Behaviour, *J. Inorg. Organomet. Polym. Mater.*, **26(1)**: 208-218 (2016).

[13] Mabrouk T.M.M., Khozemy E.E., Ali A.E.H., Investigating the Electrical and Thermal Characteristics of Bismuth/(Polyvinyl alcohol/Acrylic Acid) Nanocomposites Membranes Prepared by Ionizing Radiation, *J. Inorg. Organomet. Polym. Mater.*, **27(2)**: 399-455 (2017).

[14] Yang C.C., Chien W.C., Li T.J., Direct Methanol Fuel Cell Based on Poly(Vinyl Alcohol)/Titanium Oxide Nanotubes/Poly(Styrene Sulfonic Acid) (PVA/Nt-TiO2/PSSA) Composite Polymer Membrane, *J. Power Sources*., **195(11):** 3407-3415 (2017).

[15] Kim D.S., Park H.B., Rhim J., Lee Y.M., Preparation and Characterization of Crosslinked PVA/SiO_2 Hybrid Membranes Containing Sulfonic Acid Groups for Direct Methanol Fuel Cell Applications, *J. Membr. Sci*., **240**: 37-48 (2004).

[16] Tsai C.E., Lin C.W., Rick J., Hwang B.J., Poly(Styrene Sulfonic Acid)/Poly(Vinyl Alcohol) Copolymers With Semi-Interpenetrating Networks as Highly Sulfonated Proton-Conducting Membranes, *J. Power Sources*, **196(13)**: 5470-(2011).

[17] Kim D.S., Cho H.I.I., Kim D.H., Lee B.S., Yoon S.W., Kim Y.S., Moon G.Y., Byun H., Rhim J., Surface Fluorinated Poly(vinyl alcohol)/poly(styrene sulfonic acid-co-maleic acid) Membrane for Polymer Electrolyte Membrane Fuel Cells, *J. Membr. Sci*., **342**: 138-144 (2009).

[18] Rhim J.W., Park H.B., Lee C.S., Jun J.H., Kim D.S., Lee Y.M., Crosslinked poly(vinyl alcohol) Membranes Containing Sulfonic Acid Group: Proton and Methanol Transport Through Membranes, *J. Membr. Sci*. **238:** 143-151 (2004).

[19] Hooshyari K.H., Javanbakht M., Adibi M., Novel Composite Membranes Based on PBI and Dicationic Ionic Liquids for High Temperature Polymer Electrolyte Membrane Fuel Cells, *Electrochim. Acta*, **205**:142-152 (2016).

[20] Hooshyari K.H., Javanbakht M., Adibi M., Novel Composite Membranes Based on Dicationic Ionic Liquid and Polybenzimidazole Mixtures as Strategy for Enhancing Thermal and Electrochemical Properties of Proton Exchange Membrane Fuel Cells Applications at High Temperature, *Int. J. Hydrogen Energy*, **41(25)**: 10870-10883 (2016).

[21] Shabanikia A., Javanbakht M., Amoli H.S., Hooshyari K.H., Enhessari M., Polybenzimidazole/ Strontium Cerate Nanocomposites with Enhanced Proton Conductivity for Proton Exchange Membrane Fuel Cells Operating at High Temperature, *Electrochim. Acta*, **154**: 370-378 (2015).

[22] Hooshyari K.H., Javanbakh, M., Shabanikia A., Enhessari M., Fabrication BaZrO3/PBI-Based Nanocomposite as a New Proton Conducting Membrane for High Temperature Proton Exchange Membrane Fuel Cells, *J. Power Sources*, **276**: 62-72 (2015).

[23] Shabanikia A., Javanbakht M., Amoli H.S., Hooshyari K.H., Enhessari, M., Effect of La2Ce2O7 on the Physicochemical Properties of Phosphoric Acid Doped Polybenzimidazole Nanocomposite Membranes for High Temperature Proton Exchange Membrane Fuel Cells Applications Fuel Cells, Electrolyzers, and Energy Conversion, *J. Electrochem. Soc.*, **161(14)**: F1403-F1408 (2014).

[24] Shabanikia A., Javanbakht M., Amoli H.S., Hooshyari K., Enhessari M., Novel Nanocomposite Membranes Based on Polybenzimidazole and Fe_2TiO_5 Nanoparticles for Proton Exchange Membrane Fuel Cells, *Ionics*, **21(8)**: 2227-2236 (2015).

[25] Attaran A.M., Javanbakht M., Hooshyari K., Enhessari M., New Proton Conducting Nanocomposite Membranes Based on Poly Vinyl Alcohol/Poly Vinyl Pyrrolidone/BaZrO3 for Proton Exchange Membrane Fuel Cells, *Solid State Ion.*, **269**: 98-105 (2015).

[26] Wu Y., Wu C., Li Y., Fu Y., PVA–silica Anion-Exchange Hybrid Membranes Prepared Through a Copolymer Crosslinking Agent, *J. Membr. Sci*, **350**: 322-332 (2010).

[27] Caetano E., de Souza C., Muccillo R., Properties and Applications of Perovskite Proton Conductors., *J. Mat. res.*, **13(3)**: 385-394 (2010).

[28] Mirfakhraei B., Ramezanipour F., Paulson S., Birss V., Thangadurai V., Effect of Sintering Temperature on Microstructure, Chemical Stability, and Electrical Properties of Transition Metal or Yb-doped BaZr0.1Ce0.7Y0.1M0.1O3−δ (M = Fe, Ni, Co, and Yb), *Frontiers in Energy Research*, **2**: 9-(2014).

[29] Ciontea L., Ristoiu T., Suciu R., Petrisor T., Neamtu B., Rufoloni A., Celentano G., Petrisor T., Chemical Processing and Characterization of Barium Zirconate Nanopowders, *J. Optolectron. Adv. Mater.*, **9(3)**: 776-779 (2007).

[30] Raiteri P., Gale J., Bussi G., Reactive Force Field Simulation of Proton Diffusion in $BaZrO_3$ Using an Empirical Valence Bond Approach, *J. Phys: Condens. Matter*, **23**: 334213 (2011).

[31] Stokes S., Saiful Islam M., Defect Chemistry and Proton-Dopant Association in $BaZrO_3$ and $BaPrO_3$, *J. Mater. Chem.*, **20**: 6258-6264 (2010).

[32] Onishi T., Helgaker T., "A Theoretical Study on Proton Conduction Mechanism in $BaZrO_3$ Perovskite", Chapter 14, Springer International Publishing Switzerland (2013).

[33] Zajac W., Rusinek D., Zheng K., Molenda J., Applicability of Gd-Doped $BaZrO_3$, $SrZrO_3$, $BaCeO_3$ and $SrCeO_3$ Proton Conducting Perovskites as Electrolytes for Solid Oxide Fuel Cells, *Cent. Eur. J. Chem.*, **11(4)**: 471-484 (2013).

[34] Cherry M., Islam M.S., Gale J.D., Catlow C.R.A., Computational Studies of Protons in Perovskite-Structured Oxides, *J. Phys. Chem.* **99(40)**: 14614-14618 (1995).

[35] Singh K., Kannan R., Thangadurai V., Synthesis and Characterisation of Ceramic Proton Conducting Perovskite-Type Multi-element-doped $Ba_{0.5}$ $Sr_{0.5}$ $Ce_{1-x-y-z}$ Zr_x Gd_y Y_z $O_{3-\delta}$ ($0 < x < 0.5$; $y = 0, 0.1, 0.15$; $z = 0.1, 0.2$), *Int. J. Hydrogen Energy*, **41(30)**: 13227-13237 (2013).

[36] Yang J., Deng L., Han C., Duan J., Ma M., Zhang X., Xu F., Sun R., Synthetic and Viscoelastic Behaviors of Silicananoparticle Reinforced Poly(acrylamide) Core-Shell Nanocomposite Hydrogels, *Soft Matter.*, **9(4)**: 1220-1230 (2013).

[37] Kumar S.K., Jouault N., Benicewicz B., Neely T., Nanocomposites with Polymer Grafted Nanoparticles, *Macromol.*, **46(9)**: 3199-3214 (2013).

[38] Li Y., Krentz T.M., Wang L., Benicewicz B.C., Schadler L.S., Ligand Engineering of Polymer Nanocomposites: from the Simple to the Complex, *ACS App. Mater. Interfaces*, **6(9)**:6005-6021 (2014).

[39] Restolho J., Serro A.P., Mata J.L., Saramago B., Viscosity and Surface Tension of 1-ethanol-3-Methylimidazolium Tetrafluoroborate and 1-methyl-3-octylimidazolium Tetrafluoroborate over a Wide Temperature Range, *J. Chem. Eng. Data*, **54(3)**: 950-955 (2009).

[40] Tokuda H., Hayamizu K., Ishii K., Susan M.A.B.H., Watanabe M., Physicochemical Properties and Structures of Room Temperature Ionic Liquids. 2. Variation of Alkyl Chain Length in Imidazolium Cation, *J. Phys. Chem. B*, **109(13)**: 6103-6110 ( ).

[41] Kim D.S., Guiver M.D., Nam S., Yun T.I., Seo M., Kim S.J., Hwang H.S., Rhim J.W., Preparation of Ion Exchange Membranes for Fuel Cell Based on Crosslinked Poly(vinyl alcohol) with Poly(styrene Sulfonic Acid-Co-Maleic Acid), *J. Membr. Sci.*, **281**: 156-162 (2006).

[42] Tsai C.E., Lin C.W., Rick J., Hwang B.J., Poly(styrene sulfonic acid)/poly(vinyl alcohol) Copolymers With Semi-Interpenetrating Networks as Highly Sulfonated Proton-Conducting Membranes, *J. Power Sources*, **196(13)**:5470-5477 (2011).

[43] Attaran A.M., Javanbakht M., Hooshyari K., Enhessari M., New Proton Conducting Nanocomposite Membranes Based on Poly Vinyl Alcohol/Poly Vinyl Pyrrolidone/$BaZrO_3$ for Proton Exchange Membrane Fuel Cells, *Solid State Ionics*, **269**: 98-105 (2015).

[44] Hooshyari K., Javanbakht M., Enhessari M., Beydaghi H., Novel PVA/$La_2Ce_2O_7$ hybrid nanocomposite Membranes for Application in Proton Exchange Membrane Fuel Cells, *Iran. J. Hydrogen & Fuel Cell.*, **1(2)**: 105-112 (2014).

[45] Huang Y.F., Chuang L.C., Kannan A.M., Lin C.W., Proton-Conducting Membranes with High Selectivity from Cross-Linked Poly(Vinyl Alcohol) and Poly(Vinyl Pyrrolidone) For Direct Methanol Fuel Cell Applications, *J. Power Sources*, **186(1)**:22-28 (2009).

[46] Hsu P.Y., Hu T.Y., Highly Zeolite-Loaded Polyvinyl Alcohol Composite Membranes for Alkaline Fuel-Cell Electrolytes, *Polymers*, **10(1)**: 102 (2018).

[47] Boroglu M.S., Cavus S., Boz I., Ata A., Synthesis and Characterization Of Poly(Vinyl Alcohol) Proton Exchange Membranes Modified with 4,4-Diaminodiphenylether-2,2-Disulfonic Acid, *EXPRESS Polymer Letters*, **5**(5): 470-478 (2011).

[48] Bahador A.R., Molaei M., Karimipour M., One-pot room temperature synthesizing Cu- and Mn-doped ZnSe nanocrystals by a rapid photochemical method, *Mod. Phys. Lett. B*, **30(11)**:1650227- 1650227 (2016).

[49] Bahador A.R., Taheri Otaqsara S.M., Baizaee S.M., A Fast, Room Temperature Excimer Laser Route for the Synthesis of Ag/MWCNT Nanocomposite Without Using Reducing Agent and Investigating Its Photoresponse Behavior to Visible Illumination, *Appl. Surf. Sci*., **457**: 1087–1095 (2018).

[50] Kang M.S., Choi Y.J., Moon S.H., Water-Swollen Cation-Exchange Membranes Prepared Using Poly(vinyl alcohol) (PVA)/poly(styrene sulfonic acid-co-maleic acid) (PSSA-MA), *J. Membr. Sci*., **207(2)**: 157-170 (2002).

[51] Baizaee S.M., Arabi M., Bahador A.R., A Simple, One-Pot, Low Temperature And Pressure Route for the Synthesis of RGO/ZnO Nanocomposite and Investigating Its Photocatalytic Activity, *Mat. Sci. Semicon. Proc*., **82**: 135-142 (2018).

[52] Arabi M., Baizaee S.M., Bahador A.R., Taheri Otaqsara S.M., Rapid, controllable, One-Pot and Room-Temperature Aqueous Synthesis of ZnO:Cu Nanoparticles by Pulsed UV Laser and Its Application for Photocatalytic Degradation of Methyl Orange, *Luminescence*, **33(3):** 475-485 (2018).